Design and Status of RERTR Irradiation Tests in the Advanced Test Reactor

D. M. Wachs[1], R. G. Ambrosek, G. S. Chang, M. K. Meyer
Idaho National Laboratory
P.O. Box 1625, Scoville, ID 83415-6188 , USA

ABSTRACT

Irradiation testing of U-Mo based fuels is the central component of the Reduced Enrichment for Research and Test Reactors (RERTR) program fuel qualification plan. Several RERTR tests have recently been completed or are planned for irradiation in the Advanced Test Reactor (ATR) located at the Idaho National Laboratory in Idaho Falls, ID. Four mini-plate experiments in various stages of completion are described in detail, including the irradiation test design, objectives, and irradiation conditions. Observations made during and after the in-reactor RERTR-7A experiment breach are summarized. The irradiation experiment design and planned irradiation conditions for full-size plate test are described. Progress toward element testing will be reviewed.

1. Introduction

An aggressive fuel development plan has been proposed for the Reduced Enrichment for Research and Test Reactor (RERTR) fuel development program. The central component of this development plan is irradiation testing under various conditions including power, burnup, temperature, scale, etc. A variety of fuel compositions and fabrication techniques continue to be evaluated in parallel to ensure that multiple paths to success exist in the event that unforeseen fuel performance issues force the abandonment of any one technology.

Seven irradiation campaigns have been completed by the RERTR program over the last decade in order to identify viable high uranium density fuel forms. These tests helped identify the excellent irradiation performance of U-Mo fuel alloys. However, chemical interactions with the standard aluminum matrix resulted in an unstable interaction layer that behaved poorly under irradiation. Several potential solutions are being evaluated to stabilize this interaction layer and/or to limit its growth. These solutions include adding silicon to the matrix or small amounts of zirconium or titanium to the fuel alloy. There are indications that these additions may stabilize the interaction layer. Another proposed solution is the elimination of the matrix altogether, the so-called monolithic fuel form. Questions of fabrication and mechanical behavior of this fuel form currently dominate fuel development activities. The near term irradiation test plans are discussed here and include the continued testing of mini-plates and a progression toward full-size plate testing.

2. RERTR-7 Experiment Descriptions

[1] Corresponding Author

The RERTR-7A and -7B experiments were the seventh and eighth test trains of similar design assembled to examine the performance of uranium-molybdenum alloy based fuels. As is typical for MTR type fuel elements, the base fuel form is nominally dispersed in an aluminum matrix, clad with Al-6061, and roll bonded. While the fuel form itself has performed exceptionally well under irradiation, extensive chemical interaction between the fuel and aluminum matrix has been observed at high temperature and burnup which has lead to undesirable swelling and, in some cases, breakaway swelling.

A number of modifications to the base fuel form have been identified that may reduce swelling and/or change the stoichiometry of the fuel/matrix interaction (and thus eliminate breakaway swelling) Alterations include the use of a modified matrix material (primarily through silicon additions), modified fuel alloy (small additions of refractory metal), and monolithic fuel meats (omission of the matrix material altogether). The modified matrix and monolithic fuel systems were successfully tested at low power and moderate burnup in the RERTR-6 experiment. Post irradiation examination is nearly complete as of July 2006 and no indications of impending failure have been identified for high silicon bearing matrix or monolithic fuels. However, plates with very low silicon content did show clear signs of extensive and interconnected porosity. The RERTR-7A experiment was designed to test U-Mo based fuel systems similar to the RERTR-6 experiments only at higher power and burnup. The RERTR-7A experiment test matrix is shown in Table 1. The RERTR-7B experiment was devised as a partner to the RERTR-7A experiment to test the performance of ternary fuel alloys in dispersion fuels. The RERTR-7B experiment test matrix is shown in Table 2.

Capsule	Column 1	Column 2	Column 3	Column 4
A-Top	A1 DUM11 BLANK	A2 DUM14 BLANK	A3 DUM12 BLANK	A4 DUM8 BLANK
A-Bottom	A5 R3R040 U-7Mo Roll Al 4043 Matrix	A6 V5R040 U-7Mo Roll Al-0.5Si Matrix	A7 R5R030 U-10Mo Roll Al-0.5 Si Matrix	A8 H1F020 U-12Mo FSW 0.010" Foil
B-Top	B1 R1R040 U-7Mo Roll Al 6061 Matrix	B2 R2R040 U-7Mo Roll Al-2Si Matrix	B3 R0R010 U-7Mo Roll Pure Al Matrix	B4 H1T010 U-12Mo TLPB 0.010" Foil
B-Bottom	B5 L1F01L U-10Mo FSW Holed Foil	B6 V5R050 U-7Mo Roll Al-0.5Si Matrix	B7 L1F140 U-10Mo FSW 0.010" Foil	B8 MZ25 U-7Mo Roll Zr Clad CNEA
C-Top	C1 H1F030 U-12Mo FSW 0.010" Foil	C2 L1T020 U-10Mo TLPB 0.010" Foil	C3 L1F110 U-10Mo FSW 0.010" Foil	C4 MZ50 U-7Mo Roll Zr Clad CNEA
C-Bottom	C5 L1F120 U-10Mo FSW 0.010" Foil	C6 H1T020 U-12Mo TLPB 0.010" Foil	C7 R3R050 U-7Mo Roll Al 4043 Matrix	C8 R5R040 U-10Mo Roll Al-0.5 Si Matrix
D-Top	D1 R1R050 U-7Mo Roll Al 6061 Matrix	D2 DUM13 BLANK	D3 R0R020 U-7Mo Roll Pure Al Matrix	D4 DUM19 BLANK
D-Bottom	D5 DUM05 BLANK	D6 L1F160 U-10Mo FSW 0.010" Foil	D7 L2F040 U-10Mo TLPB 0.020" Foil	D8 R2R050 U-7Mo Roll Al-2Si Matrix

Table 1. RERTR-7A test matrix.

Capsule	Column 1	Column 2	Column 3	Column 4
A-Top	A1 DUM67 BLANK	A2 DUM61 BLANK	A3 DUM75 BLANK	A4 DUM58 BLANK
A-Bottom	A5 DUM74 BLANK	A6 DUM56 BLANK	A7 DUM54 BLANK	A8 DUM53 BLANK
B-Top	B1 DUM65 BLANK	B2 DUM57 BLANK	B3 DUM48 BLANK	B4 DUM62 BLANK
B-Bottom	B5 DUM68 BLANK	B6 DUM82 BLANK	B7 DUM63 BLANK	B8 DUM72 BLANK
C-Top	C1 F3R010 U-7Mo-2Zr Roll Al-4043	C2 R0R010 U-7Mo Roll Al	C3 R3R010 U-7Mo Roll Al-4043	C4 D3R010 U-7Mo-1Ti Roll Al-4043
C-Bottom	C5 DUM59 BLANK	C6 DUM66 BLANK	C7 DUM83 BLANK	C8 DUM55 BLANK
D-Top	D1 DUM71 BLANK	D2 DUM60 BLANK	D3 DUM50 BLANK	D4 DUM64 BLANK
D-Bottom	D5 DUM49 BLANK	D6 DUM73 BLANK	D7 DUM52 BLANK	D8 DUM51 BLANK

Table 2. RERTR-7B test matrix.

The RERTR mini-plate test trains consist of 32 mini-plates assembled into 4 capsules (8 mini-plates per capsule). Not all mini-plates contain fuel. Schematics of a plate and capsule are shown in Figures 1 and 2. The capsules are stacked vertically in a basket and are cooled by direct contact with ATR primary coolant. Each mini-plate fuel meat contains approximately 6 grams of uranium. The uranium enrichment was set to 58% U-235 to control the power density in the fuel. The dispersion and monolithic fuel meat volumes are roughly 1.0 cc and 0.4 cc, respectively. Flow velocities over the plates are 10 and 14 ft/sec for outer and inner channels, respectively. The estimated beginning of life thermal conditions are described in Tables 3 and 4. The average burnups were between 50 and 90% LEU equivalent at the end of the irradiation.

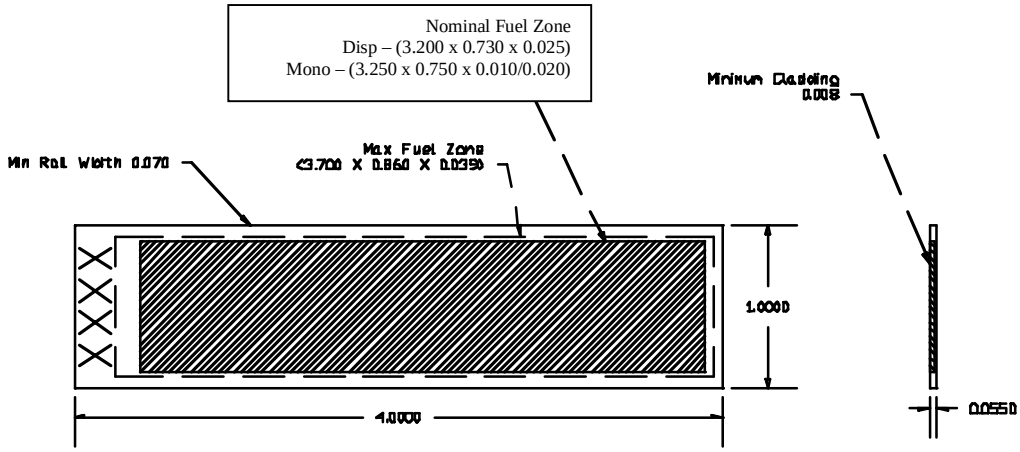

Figure 1. RERTR mini-plate.

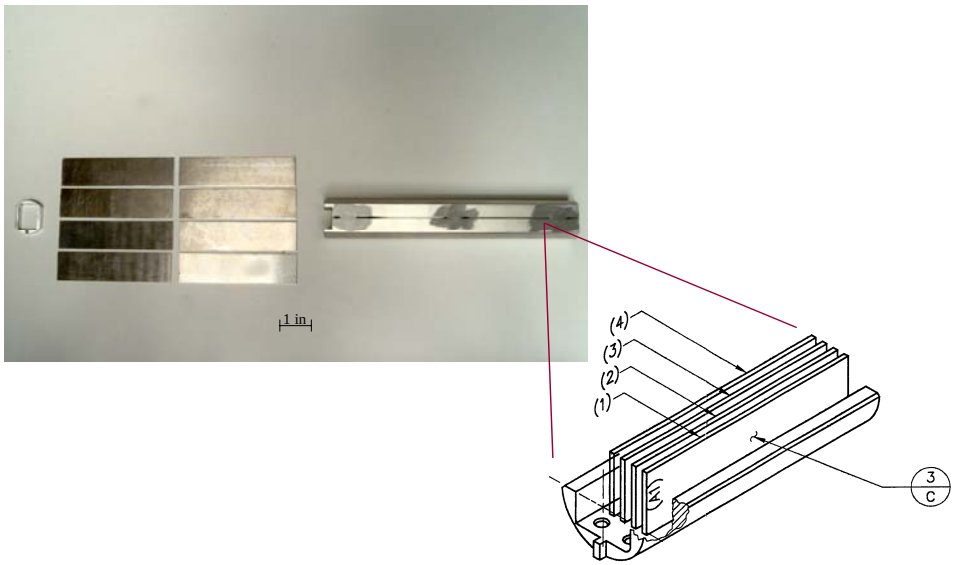

Figure 2. RERTR mini-plate capsule.

Fuel Plate	Fuel Type	Fuel Form	Heat Flux (W/cm2)	Fuel Plate Power (W)	Coolant Temp. (°C)	Plate Surf. Temp. (°C)	Clad Surf. Temp. (°C)	Fuel-Clad Interf. Temp. (°C)	Fuel Cent. Temp. (°C)
A-1	blank	-n/a-	0	0	52	52	52	52	52
A-2	blank	-n/a-	0	0	52	52	52	52	52
A-3	blank	-n/a-	0	0	52	52	52	52	52
A-4	blank	-n/a-	0	0	52	52	52	52	52
A-5	U-7Mo	disp	260	9375	54	91	97	103	130
A-6	U-10Mo	disp	215	7774	54	85	89	95	117
A-7	U-7Mo	disp	217	7849	54	85	90	95	118
A-8	U-12Mo	foil	240	8674	54	88	94	102	109
B-1	U-7Mo	disp	292	10554	57	99	106	113	144
B-2	U-7Mo	disp	242	8732	57	92	97	103	129
B-3	U-7Mo	disp	243	8764	57	92	97	103	129
B-4	U-12Mo	foil	269	9703	57	96	102	111	119
B-5	U-10Mo	foil	265	9558	61	98	104	114	121
B-6	U-10Mo	disp	235	8491	61	94	99	105	130
B-7	U-10Mo	foil	174	6280	61	85	89	96	100
B-8	U-7Mo	foil	127	4595	61	79	82	86	90
C-1	U-12Mo	foil	268	9662	64	102	108	117	125
C-2	U-10Mo	foil	164	5907	64	87	91	96	101
C-3	U-10Mo	foil	235	8479	64	97	102	111	117
C-4	U-7Mo	thick foil	209	7539	64	93	98	104	115
C-5	U-10Mo	foil	289	10414	67	108	115	125	133
C-6	U-12Mo	foil	226	8169	67	99	104	112	119
C-7	U-7Mo	disp	249	8982	67	102	108	114	140
C-8	U-7Mo	disp	298	10769	67	110	116	123	155
D-1	U-7Mo	disp	322	11636	70	116	123	131	165
D-2	blank	-n/a-	0	0	70	70	70	70	70
D-3	U-7Mo	disp	324	11678	70	116	123	131	165
D-4	blank	-n/a-	0	0	70	70	70	70	70
D-5	blank	-n/a-	0	0	72	72	72	72	72
D-6	U-10Mo	foil	192	6945	72	100	104	111	116
D-7	U-10Mo	thick foil	297	10720	72	115	121	130	146
D-8	U-7Mo	disp	234	8445	72	106	111	117	141

Table 3. BOL thermal conditions for RERTR-7A.

Fuel Plate	Fuel Type	Fuel Form	Heat Flux (W/cm2)	Fuel Plate Power (W)	Coolant Temp. (°C)	Plate Surf. Temp. (°C)	Clad Surf. Temp. (°C)	Fuel-Clad Interf. Temp. (°C)	Fuel Cent. Temp. (°C)
A-1	blank	-n/a-	0	0	52	52	52	52	52
A-2	blank	-n/a-	0	0	52	52	52	52	52
A-3	blank	-n/a-	0	0	52	52	52	52	52
A-4	blank	-n/a-	0	0	52	52	52	52	52
A-5	blank	-n/a-	0	0	52	52	52	52	52
A-6	blank	-n/a-	0	0	52	52	52	52	52
A-7	blank	-n/a-	0	0	52	52	52	52	52
A-8	blank	-n/a-	0	0	52	52	52	52	52
B-1	blank	-n/a-	0	0	53	53	53	53	53
B-2	blank	-n/a-	0	0	53	53	53	53	53
B-3	blank	-n/a-	0	0	53	53	53	53	53
B-4	blank	-n/a-	0	0	53	53	53	53	53
B-5	blank	-n/a-	0	0	53	53	53	53	53
B-6	blank	-n/a-	0	0	53	53	53	53	53
B-7	blank	-n/a-	0	0	53	53	53	53	53
B-8	blank	-n/a-	0	0	53	53	53	53	53
C-1	U-7Mo-2Zr	disp	234	8453	54	88	93	99	124
C-2	U-7Mo	disp	192	6937	54	82	86	91	111
C-3	U-7Mo	disp	191	6900	54	82	86	91	111
C-4	U-7Mo-1Ti	disp	234	8445	54	88	93	99	123
C-5	blank	-n/a-	0	0	56	56	56	56	56
C-6	blank	-n/a-	0	0	56	56	56	56	56
C-7	blank	-n/a-	0	0	56	56	56	56	56
C-8	blank	-n/a-	0	0	56	56	56	56	56
D-1	blank	-n/a-	0	0	56	56	56	56	56
D-2	blank	-n/a-	0	0	56	56	56	56	56
D-3	blank	-n/a-	0	0	56	56	56	56	56
D-4	blank	-n/a-	0	0	56	56	56	56	56
D-5	blank	-n/a-	0	0	56	56	56	56	56
D-6	blank	-n/a-	0	0	56	56	56	56	56
D-7	blank	-n/a-	0	0	56	56	56	56	56
D-8	blank	-n/a-	0	0	56	56	56	56	56

Table 4. BOL thermal conditions for RERTR-7B.

2.1 Irradiation History

The RERTR-7A experiment was inserted on November 24, 2005 and was irradiated in the ATR B-11 position through the end of cycle 136A without incident (a total of 51 days ending January 14, 2006). After the cycle, the experiment was moved from the reactor to the canal for short-term storage during the 6 day outage. The experiment was then reinserted into the ATR B-11 position for cycle 136B. The RERTR-7B experiment was first inserted into the ATR B-12 position for this cycle as well. Cycle 138B was interrupted by a reactor SCRAM on February 13 due to a failure of the backup diesel generator and was restarted on February 19. Fuel leakage was first identified on February 23 by the recognition of elevated activity using the Real Time Monitor (RTM) located at the ATR stack. Cycle 136B was again interrupted by a reactor SCRAM on March 9 due to an interruption in commercial power. The RERTR-7A irradiation history is summarized in Table 5.

The ATR stack activity was monitored closely throughout the event to assess the extent of the leak. The ATR stack monitor activity as a function of time is shown in Figure 3. Gas samples were collected daily and analyzed to track content. The total stack activity was very strongly dominated by Ar-41, Xe-133, and Xe-135, all of which are high yield fission products. The stack emission activity appeared to peak at ~40 Ci/day on February 25 and then leveled off at approximately ~22 Ci/day for the remainder of the cycle. Flattening of the release rate suggests that the amount of exposed fuel had stabilized and stack activity was being driven by the release of fresh fission gases from the plate as they were being produced.

Cycle	Date	EFPD (total)	Notes:
136A			
Start of cycle	Nov 24, 2005	0 (0)	
End of cycle	Jan 14, 2006	51 (51)	
136B			
Start of cycle	Jan 20, 2006	0 (51)	
Scram 1	Feb 13, 2006	22 (73)	Scram due to failure of backup diesel power
Restart of cycle	Feb 19, 2006	22 (73)	
	Feb 20, 2006	23 (74)	First indications of fuel failure observed at stack gas monitor
Scram 2	Mar 9, 2006	39 (90)	Scram due to commercial power interruption
End of cycle	Mar 9, 2006	39 (90)	

Table 5. RERTR-7A irradiation history.

The on-line diagnosis of fuel failures is an area of great importance to the commercial light water reactor community and techniques developed to monitor these reactor systems can be applied to this case. BWR operators typically monitor the stack noble gas composition to identify the presence of a cladding breach and to, in some cases, evaluate the type of breach. By examining the relative amounts of each gaseous isotope at the stack, a qualitative estimation of the fission product release mechanism can be made. The measured activity of each isotope can be corrected to represent the fissions per second required to produce it by dividing the measured stack activity (in Ci/sec) by the isotope's decay constant (1/sec) and fission yield. The fissions/sec are then plotted against the decay constant for each isotope on a log-log plot.

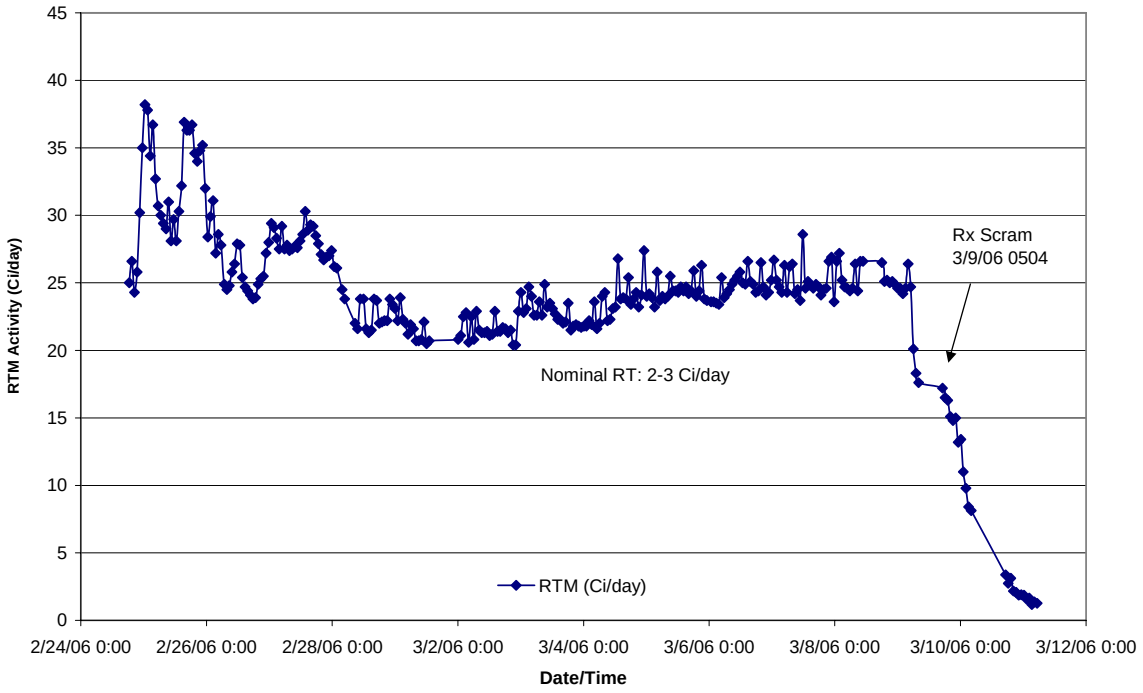

Figure 3. ATR stack activity.

Under ideal conditions the fission gases generated in tramp uranium are immediately released into the coolant and are quickly measured at the stack. In this case the plot is a horizontal line because all the fission products are produced by the same fission events and are therefore in sync. In reality though, these processes (i.e. diffusion out of the fuel particle and transport to the stack) take a finite amount of time and a portion of the shorter lived isotopes decay away before being observed at the stack. The plot is therefore typically skewed in favor of the longer lived isotopes. If the transport time constant is known the data can be corrected and the nominal fission product release rate from tramp uranium can be estimated.

Once the normal operating conditions have been established, the reactor fuel can be evaluated for cladding breaches on-line even if the total stack activity appears unchanged. The release of fission products from a fuel plate is typically restricted by diffusion through the fuel meat and the cladding breach, leading to a noticeable increase in the characteristic fission product release time constant. The total stack activity consequently becomes more dominated by the longer lived isotopes and a marked increase in slope is observed. A power law curve can be fit to the data and, in many cases, the exponent of the function can be used to diagnose the type of failure (large exponents are consistent with pin hole failures and small exponents with exposed fuel).

The data collected by the ATR RML from November 2, 2005 until March 8, 2006 is plotted in Figure 4. Measurements of each isotope are essentially constant prior to February 20, 2006 (the first measurement following the unplanned reactor scram of February 13, 2006). The normal gross stack activity was noticeably exceeded on February 23, 2006, which first alerted ATR operations to the likely breach. However, closer analysis shows that a clear change in source had already occurred on February 20, 2006. It is also important to note that the February 20 data was taken at low power and the data points were scaled to compare with the data collected at full power [1]. When this is done the presence of a breached plate becomes clear. Ultimately, this information confirms that the timing of the breach coincided with the unplanned reactor scram and that the two are likely related.

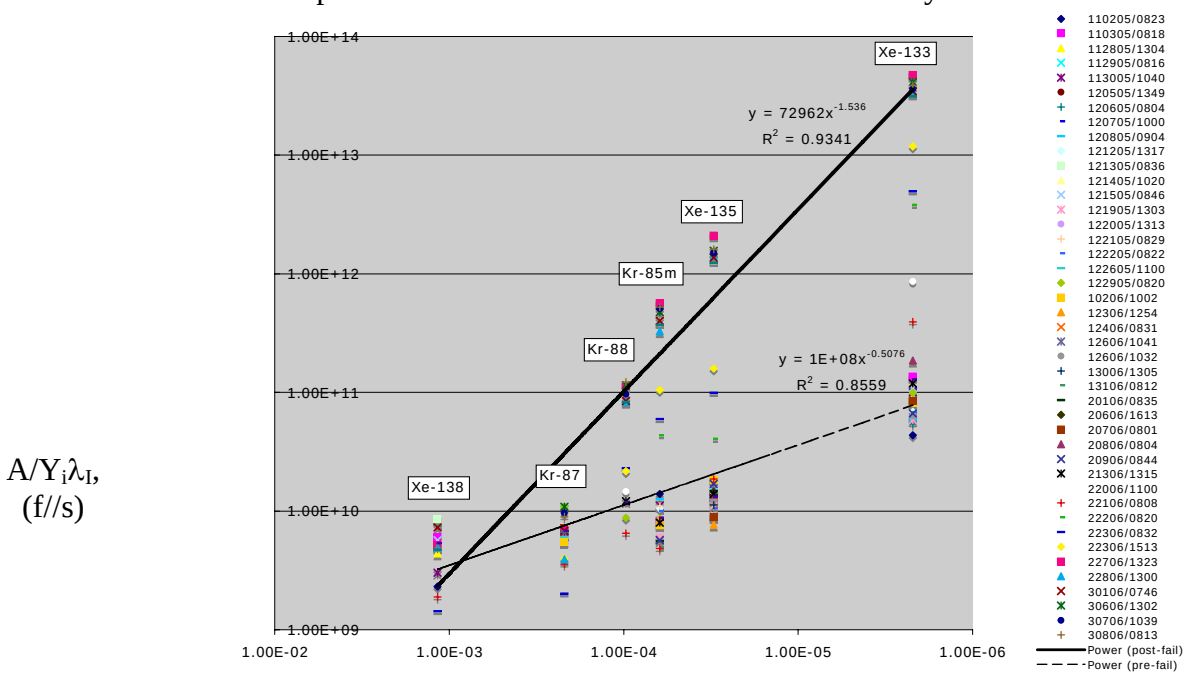

Figure 4. Analysis of release rate (fissions/second) vs. decay constant (1/second) for noble gases measured at the ATR stack.

The ATR primary coolant activity was also regularly monitored throughout the event. The measured activity levels as a function of time are shown in Figure 5. The initial increase in activity level implies that fuel and/or fission products were being washed from the failed fuel plate(s) for the first several days. A moderate increase in activity occurred over the last ten days of irradiation, suggesting that the source of additional activity was probably due to the release of new fission products rather than additional fuel loss. The total rate of release is obscured without knowledge of the ATR demin bed conditions, which should be capturing released solid particulate matter during operation. Coolant samples (540 ml) were collected and analyzed for uranium isotopics at both the RTC Radiation Measurements Laboratory and MFC Analytical Laboratory. The results are summarized in Table 6. The table shows the U-235 and U-238 concentrations found in samples taken during the event (tap water was also analyzed as a point of reference). The effective enrichment of the uranium found in the coolant was then calculated and corrected by subtracting the nominal U-235 content measured during normal operation. The corrected value should represent the effective enrichment of the leaking element.

Additional coolant samples (540 ml) were collected and strained through a filter to yield a coolant particulate sample from each reactor quadrant. The filter material was examined by the MFC Analytical Laboratory to establish content. The samples were analyzed using gamma spectrometry and ICP-MS to establish the dominant radionuclides and the uranium isotopics. This analysis further demonstrated that the coolant activity was dominated by fresh fission products.

The isotopics of uranium contained in the coolant samples were used to help identify the source of the apparent ATR stack and coolant activity. The only candidate sources in the reactor in this range of enrichment (~50% U-235) were the RERTR-7A and -7B experiments and they were therefore assumed to be the most likely source. On March 12 a soak test was performed on both RERTR experiments in the ATR canal to confirm this suspicion.

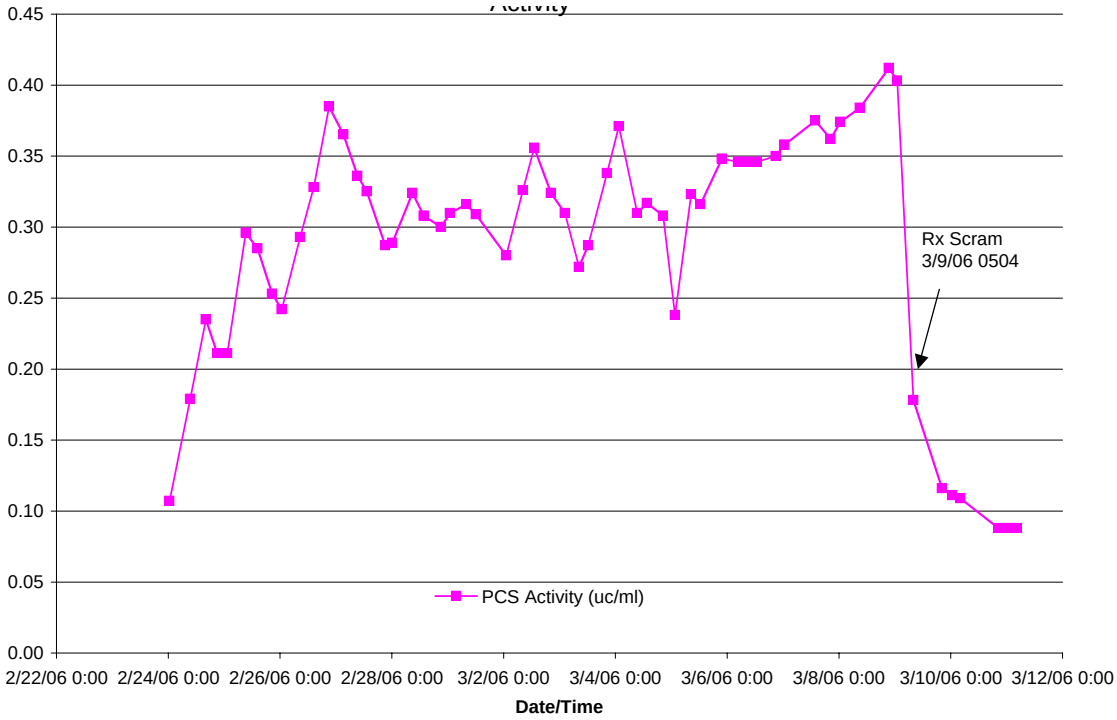

Figure 5. ATR coolant activity levels.

	U-235 (pg/ml)	U-238 (pg/ml)	Enrichment (% U-235)	Corrected Enrichment (% U-235)
RTC-RML				
Tap 1	12.36 +/- 0.25	1558 +/- 17.60	0.787 (0.812-0.763)	
Tap 2	11.62 +/- 0.21	1522 +/- 21.25	0.758 (0.782-0.734)	
Feb 20	0.51 +/- 0.03	--		
Feb 27	18.13 +/- 1.83	13.78 +/- 0.58	56.8 (60.2-53.2)	56.1 (59.6-52.4)
Mar 1	8.91 +/- 2.07	7.93 +/- 2.32	52.9 (66.2-40.0)	51.4 (65.1-38.2)
Mar 6	10.72 +/- 1.88	7.31 +/- 2.33	59.5 (71.7-47.8)	58.3 (70.8-46.4)
Mar 8	6.43 +/- 2.74	5.50 +/- 2.39	53.9 (74.7-31.9)	51.8 (73.6-28.7)
Mar 13	5.09 +/- 0.49	3.86 +/- 0.25	56.9 (60.7-52.8)	54.3 (58.4-49.9)
MFC Al*				
Mar 2	20 +/- 4	10 +/- 5	67 (83-52)	66 (82-51)

* relatively high uncertainty at low uranium concentrations is driven by high uranium background levels in the instrument

Table 6. Measured ATR coolant uranium isotopics.

Soak tests were performed by inserting the entire test train into a closed container in the canal. The container was sealed and water was thoroughly purged through the system. The experiment was soaked for 30 minutes prior to water sampling. Five samples were collected and analyzed; 1) prior to experiment handling (for reference), 2) containing the RERTR-7B experiment, 3) after purging the container upon removal of the RERTR-7B experiment, and 4) while containing the RERTR-7A experiment, and 5) a second backup sample from the RERTR-7A experiment. Each sample was analyzed using gamma spectroscopy at the RTC RML and the results are shown in Figure 6. The chart shows that no meaningful change in radionuclide content was observed when the RERTR-7B experiment was examined and that a substantial increase in activity was observed when the RERTR-7A experiment was inserted. This conclusively showed that the RERTR-7A experiment had breached at least one mini-plate and that the RERTR-7B experiment was intact. The RERTR-7A experiment was then packaged in a sealed bucket in the ATR canal to limit the spread of contamination prior to shipment for post irradiation examination.

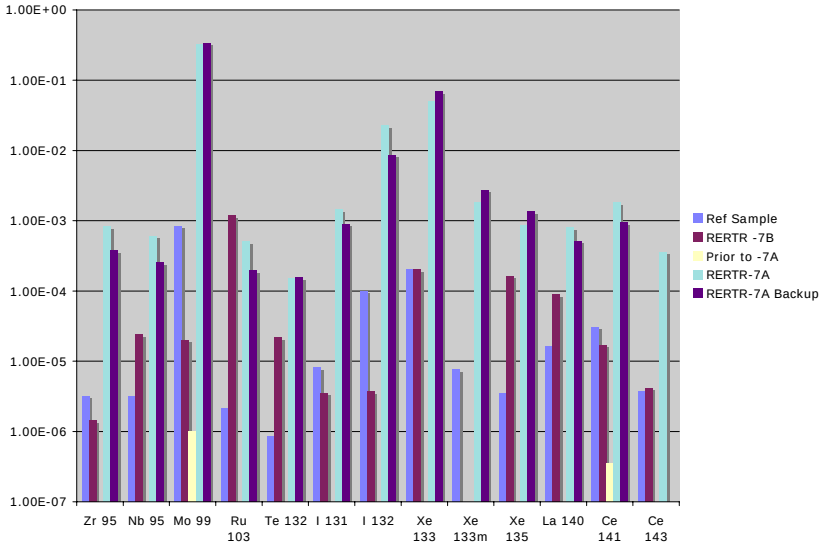

Figure 6. Soak test results showing a significant increase in µCi/ml of various radionuclides while containing the RERTR-7A experiment.

To further narrow the search for the location of the breach and to simplify transport, each capsule in the RERTR-7A experiment was individually soak tested (on May 2 and 3). Each capsule was removed from the storage bucket, placed individually in an RERTR irradiation basket, and inserted into the soak tester. The capsule was then soaked for 50 minutes and a water sample was collected. Gamma scanning results for each sample are shown in Figure 7. The activity levels observed in the RERTR-7A-A, -B, and –D capsules are all very similar and in agreement with those measured for the RERTR-7B experiment. Relative activity (e.g. relative to the activity measured for capsule A) levels from the RERTR-7B-C capsule sample, however, are an order of magnitude higher for several of the longer lived fission products (e.g. Zr-95, Nb-95, Ru-103, La-140, Ba-140, Ce-141, and Ce-143), indicating that the breached mini-plate(s) is contained in the –C capsule. The –C capsule was therefore returned to isolated storage and the –A, -B, and –D capsule were prepared for shipment to the Hot Fuel Examination Facility for PIE. The four intact capsules were subsequently packaged and shipped to the HFEF for PIE in June. The RERTR-7A-C capsule remained in the ATR canal and is transported to HFEF in early November.

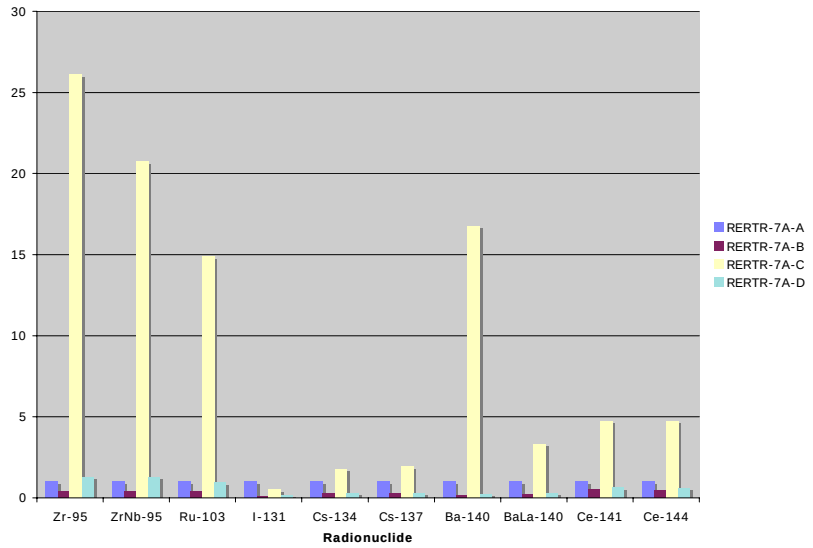

Figure 7. Individual soak test results showing significantly elevated activity from the RERTR-7A-C capsule relative to the other three capsules.

2.2 Post-Shutdown Observations at the ATR

Following the end of cycle 135C on March 9, emphasis shifted from identifying the failed element to monitoring the primary system activity levels and preparing the ATR for restart. The reactor coolant flow was stopped to enable maintenance, after which samples drawn from the primary coolant stream showed a clear drop in activity. This drop, however, was coincident with a sharp increase in activity in specific plant locations. It appeared that the activity had, in general, concentrated in areas of low flow where particulate matter may be expected to accumulate.

Prior to restart the reactor fuel was replaced by dummy elements and the primary system was operated in 3 pump mode to dislodge particulate. The primary coolant was filtered through the bypass demineralization system during this period. A substantial drop in primary coolant activity was achieved after a couple days recirculation. However, locations within the reactor that were not exposed to flowing coolant (primarily the overflow tanks) did not experience a reduction in activity. Activity in these areas will remain high until the fission products decay away over time.

2.3 Comparison with Previous Breach (RERTR-5)

The RERTR-5 experiment was inserted into a Large B-position of the ATR for cycle 123B on August 19, 2000. The experiment used flow-through capsules virtually identical to that used in the RERTR-7A experiment and was thus directly cooled by ATR primary coolant water. A breach of plate Q8003I that occupied position A-8 in the RERTR-5 experimental assembly was identified during PIE. A slight increase in coolant and stack activity was noted by ATR operations on August 29, 10 days after start of irradiation. Activity decreased to normal levels after approximately two weeks. Irradiation of RERTR-5 continued for 106 days, through the remainder of cycle 123B and cycles 123C and 124A without recognizable additional activity increase. However, RTM and PCS data were not archived due to a transition in computer platform during this timeframe. These observations must therefore be considered anecdotal. Total irradiation time for RERTR-5 was 116 EFPD's.

As was recognized for the RERTR-7A experiment, additional information about the breach can be unearthed by examining the stack gas composition. ATR stack gas analysis data collected from the start of cycle 123B (August 20, 2000) to the end of cycle 123B (November 11, 2000) is shown in Figure 8. Stack gas composition on the first day at full power is very similar to that observed in RERTR-7A before the breach, but, much like RERTR-7A, the failure is clearly evident (August 21, 2000) days before it was recognized with the Real Time Monitor at the stack and continues to be visible after the RTM values are reported to have dropped back to normal levels.

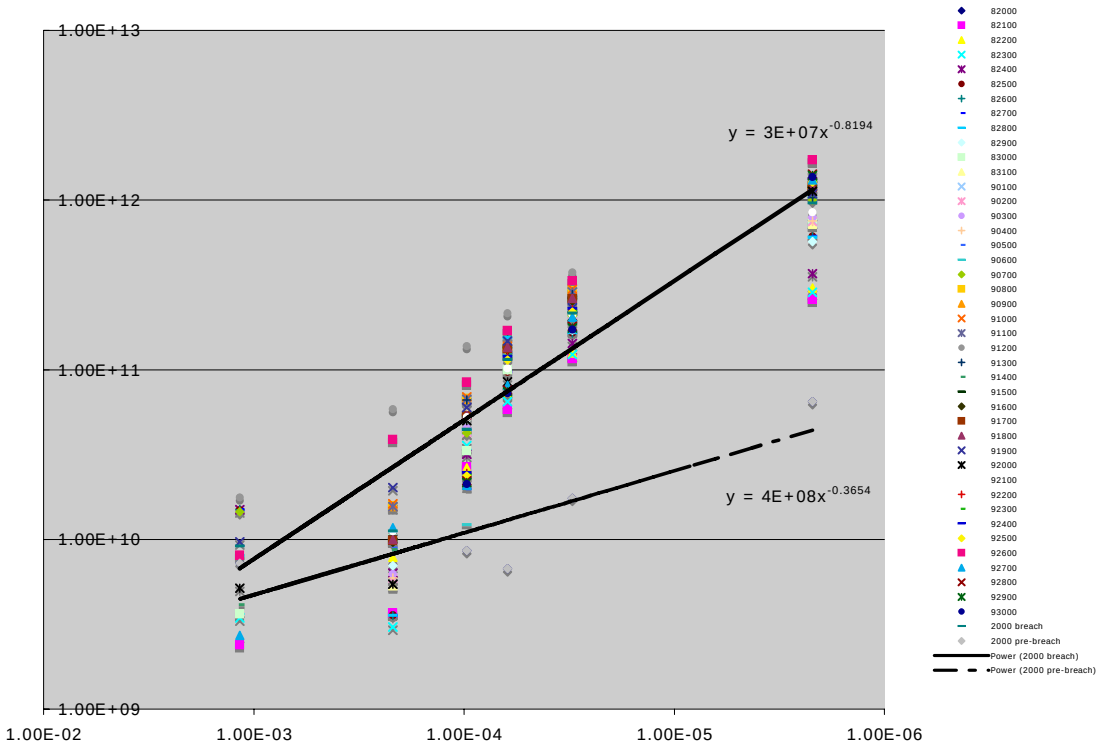

Figure 8. ATR stack gas composition analysis during the RERTR-5 experiment breach.

Operating experience in the LWR community [1,2] has shown that the exponent of the power law fit to this data can yield insight into the nature of the cladding breach. Exponents in the range of 0.5 to 1.5 have been regularly observed where 0.5 is indicative of a tramp source, 1.5 is a tight, pin-hole type breach, and 1.0 is an open breach. The exponent is not influenced by the total release from the fuel.

Small exponents are linked to large breaches because they are observed when the time between fission product formation and detection at the stack is relatively short. Tramp uranium fission is assumed to occur in the coolant and the time constant associated with detection is driven by transport from the core to the stack. Fission products escaping through an open breach into the coolant must first escape the fuel meat within the plate before being transported to the stack. This adds an additional amount of time in which the shorter lived isotopes are decayed and the exponent is thus more dominated by the longer lived isotopes. For a tight breach the fission products must first migrate out of the fuel meat and then through a narrow defect in order to reach the coolant stream. The time required to complete this journey further skews the observed stack activity toward longer lived isotopes and increases the exponent.

The power law fits for pre- and post-failure stack gas analysis results are shown for both the 2000 RERTR-5 breach and 2006 RERTR-7A breach in Figure 9. The pre-breach curves are similar in both cases and have exponents of 0.37 and 0.51 representing the contribution of tramp uranium. A time-to-detection value of roughly 4 hours was applied to the raw data as shown in Figures 5 and 9 so that these values would be consistent with values reported in the literature for BWRs and exponents for various breached conditions could be directly compared. The RERTR-5 breach exponent is roughly 0.82, which is typically representative of an open defect, while the RERTR-7A breach shows a much larger exponent of 1.5 typically indicative of a tight defect. The analogy to BWR fuel failures is, however, slightly flawed. The transport of fission products from the fuel to the coolant is primarily limited by movement through the cladding because the release rate from the fuel is largely independent of the cladding conditions. In the case of a breached plate type fuel the release rate can be dominated by either the breach characteristics or the fuel meat characteristics.

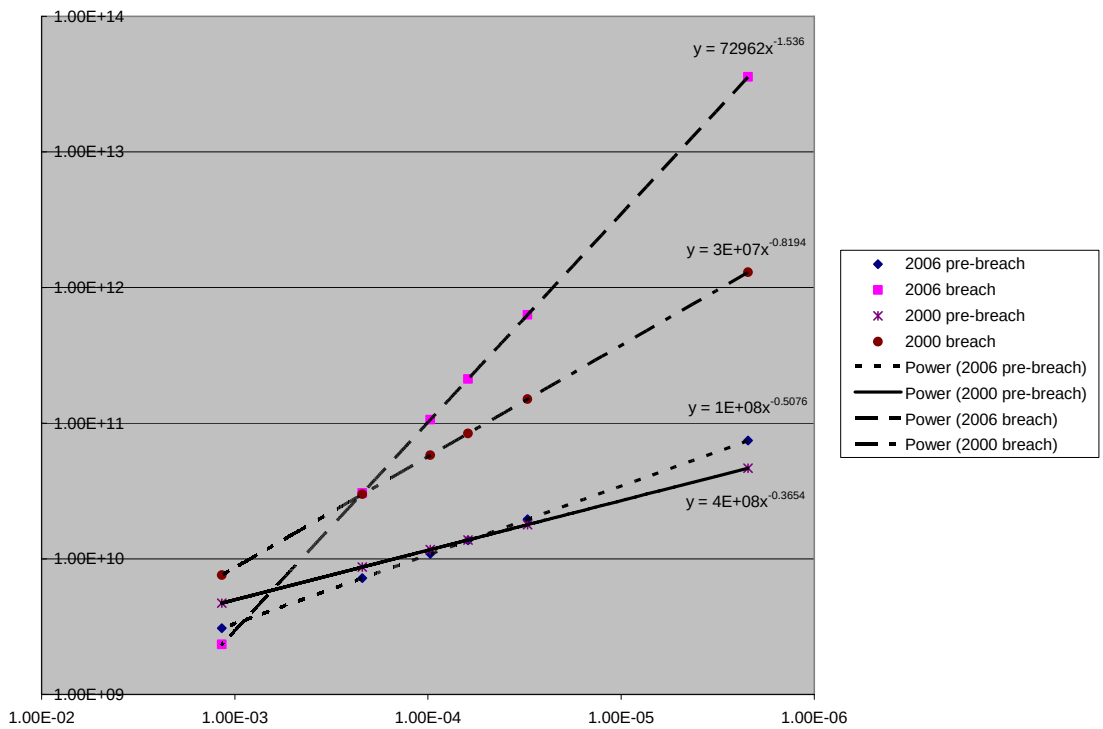

Figure 9. RERTR-6 and -7A stack gas analysis trendlines.

Post-irradiation examination showed that RERTR-5 stack activity was caused by a small crack in a thin cladding region (i.e. a fabrication defect) as shown in Figure 10. A clear stain appears on the plate

downstream of the cladding breach. The irradiation history of the plate is summarized in Table 7 and the thermal and burnup conditions in Table 8.

The difference in the quantity of fission products released can be primarily attributed to the physical state of the plate and its power level. The relative amount of fuel meat actively exposed to the breach can be estimated based on the calculated fission rates required to yield the observed fission products. The RERTR-5 and -7A experiments required ~$1x10^{12}$ and ~$3x10^{13}$ fissions/sec, respectively, to generate the observed amount of Xe-133 (the longest lived isotope) and the fission rate densities for each breached mini-plate were approximately $2.5x10^{14}$ and $1.2x10^{14}$ fissions/cc/sec. The minimum volume of fuel meat actively affected by each breach is therefore on the order of 0.01 cc and 0.10 cc for the RERTR-5 and -7A mini-plates, respectively, such that at least 10 times more of the fuel meat is affected by the breach in RERTR-7A than in RERTR-5. By examining the same effect for the shortest lived isotope (Kr-85m) where the activity is ~$1.5x10^{10}$ and $6.1x10^{9}$ it can be estimated that the active fuel volumes are $2.5x10^{-5}$ cc and $1.2x10^{-4}$ cc for the RERTR-5 and -7A experiments, respectively. The RERTR-5 experiment therefore had roughly 5 times more fuel that could be considered very close to the breach.

Comparison of the fuel meat volumes actively coupled to the breach suggests that the fuel exposure in the RERTR-5 experiment was very localized. In other words, the fission products were only released from regions very near the fractured surfaces and the remaining fuel particles remained well contained within the matrix material. The micrograph shown in Figure 11, taken very near the breach, shows the limited loss of material experienced by the RERTR-5 mini-plate. It also shows that the fuel meat stayed largely intact and only discrete surfaces were exposed rather than the entire fuel meat.

The stack gas analysis suggest that the RERTR-7A experiment, in contrast, appears to have exposed a large amount of fuel that was modestly contained within the fuel plate. Visual examination of the RERTR-7A-C capsule in the ATR canal revealed the formation of cracks along the edge of two plates. Photographs of the plates are shown in Figures 12 and 13. Both cracked plates were fabricated by transient liquid phase bonding (TLPB). Although the cause of the breach is still under investigation, a brittle, silicon rich phase was observed to form at the clad-clad bond line and it appears that this may have significantly weakened the interfacial bond.

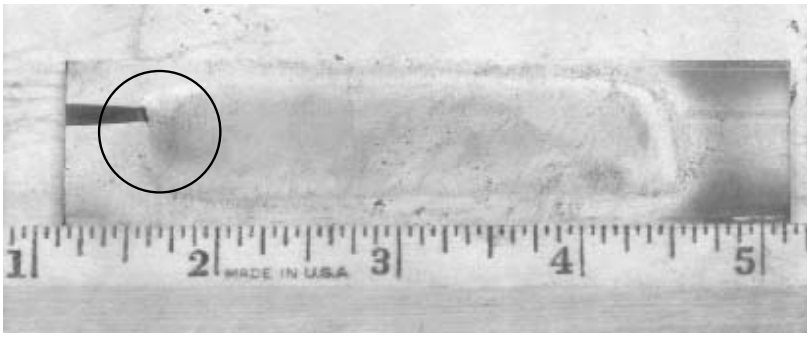

Figure 10. Breached mini-plate from RERTR-5 experiment.

Cycle	Date	EFPD (total)	Notes:
123B			
Start of cycle	Aug 19, 2000	0 (0)	
	Aug 29, 2000	10 (10)	First indications of fuel failure observed at stack gas monitor
	~Sept 12, 2000	34 (34)	Stack gas monitor levels return to normal
End of cycle	October 1, 2000	44 (44)	
123C			
Start of cycle	October 28, 2000	0 (44)	
End of cycle	November 11, 2000	14 (58)	
124A			
Start of cycle	November 17, 2000	0 (58)	
End of cycle	January 13, 2001	58 (116)	

Table 7. Irradiation history of the RERTR-5 experiment.

	EFPD	Burnup (% U235)	Power Density (W/cm^3)	Surface Heat Flux (W/cm^2)
123B				
BOC	14 (14)	4.9	3773	120
MOC	28 (28)	9.5	3568	113
EOC	42 (42)	14.0	3445	109
123C				
BOC	4.5 (48.5)	15.7	3497	111
MOC	9 (53)	17.3	3450	110
EOC	13.4 (57.4)	18.9	3404	108
124A				
BOC	19.2 (77.2)	26.5	4230	134
MOC	38.3 (96.3)	33.5	3969	126
EOC	57.5 (115.5)	40.0	3707	118

Table 8. Thermal and burnup/depletion history of the Q8003I mini-plate in the RERTR-5 experiment.

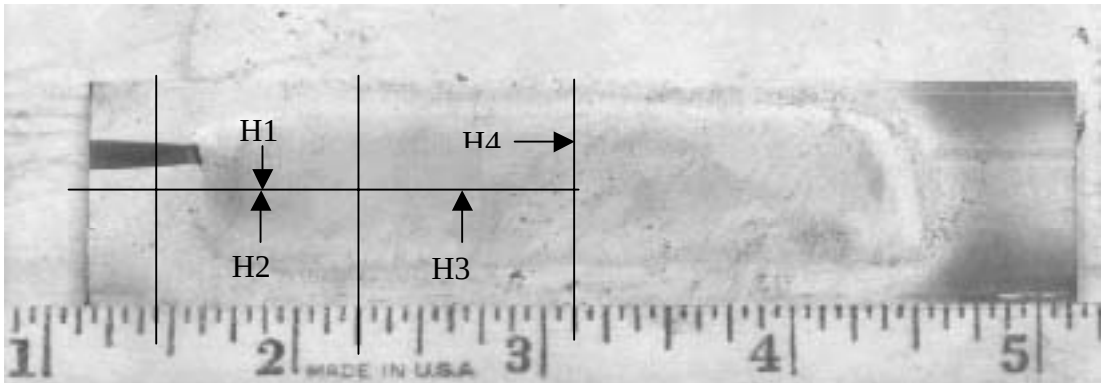

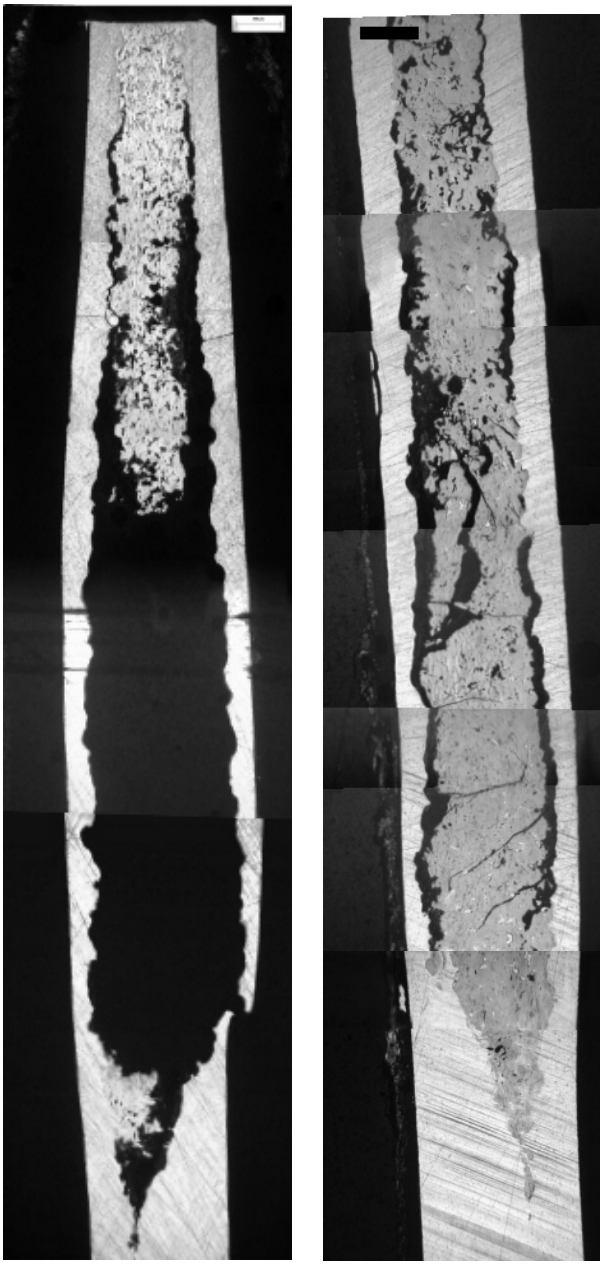

Figure 11. Optical image of the breached region of plate Q8003I from the RERTR-5 experiment. (images show section H1 on the left and section H2 on the right). The large void in the left image is likely due to fuel meat pullout during sample preparation.

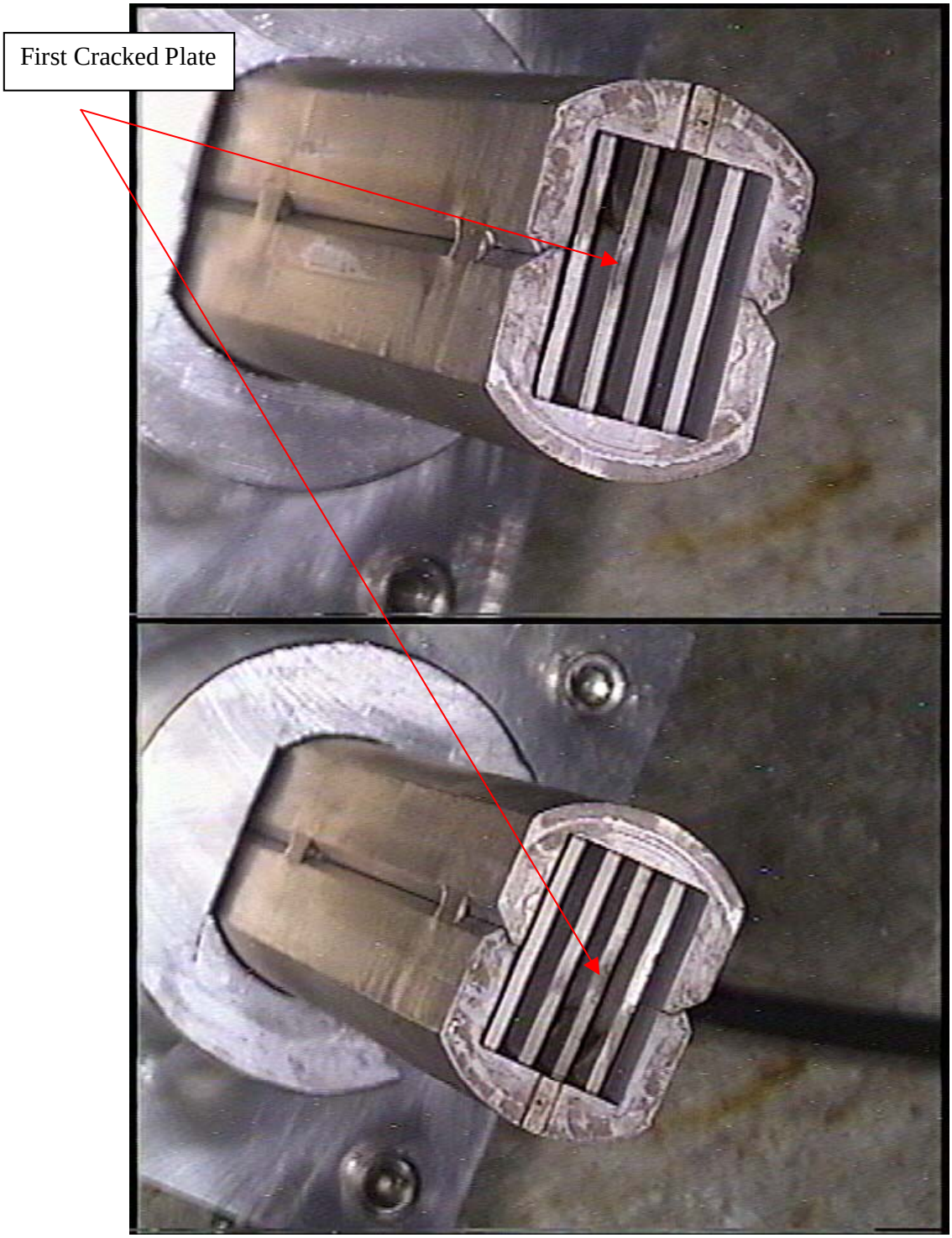

Figure 12. RERTR-7A-C capsule bottom (shown from two angles).

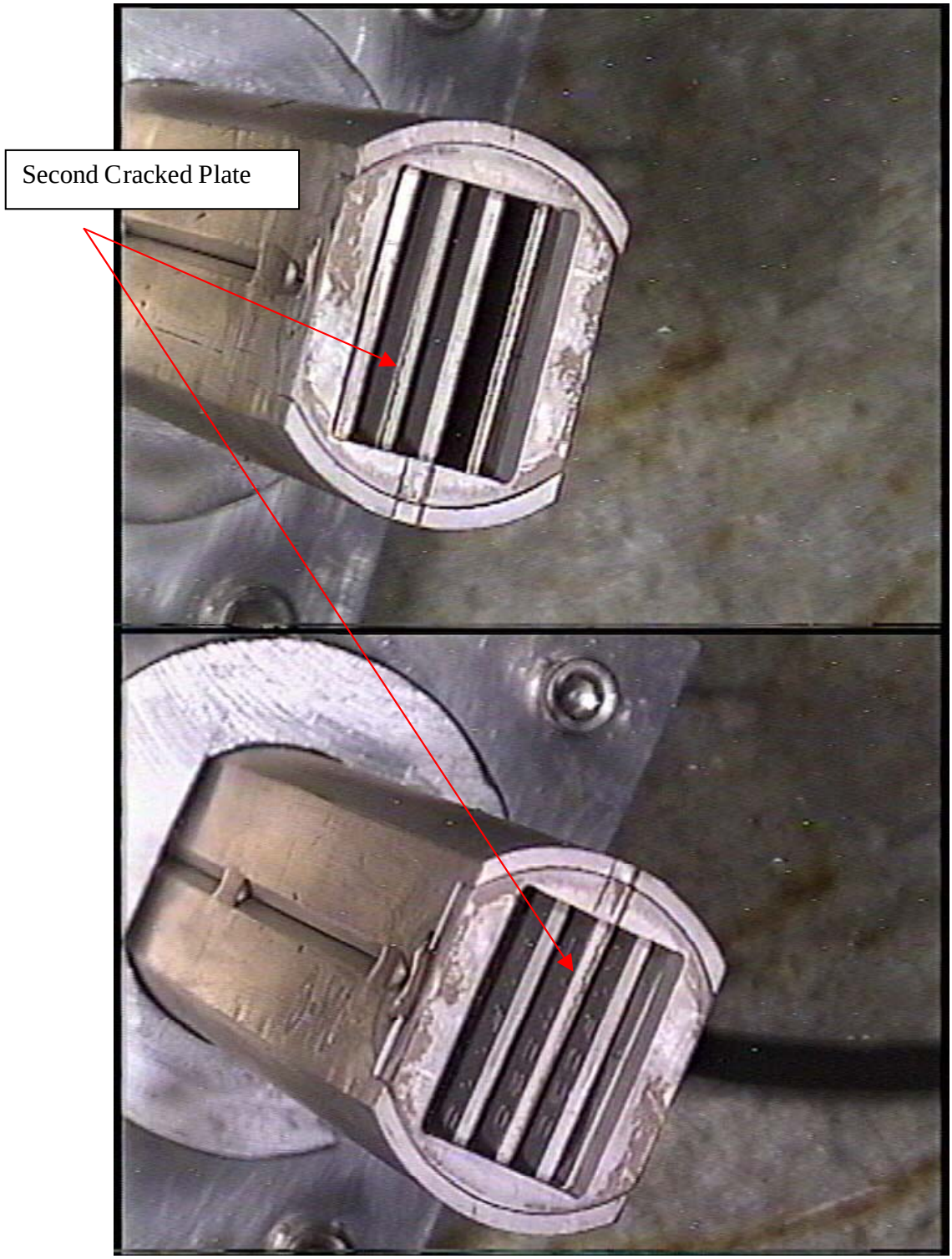

Figure 13. RERTR-7A-C capsule top (shown from two angles).

2.3 Discussion and Conclusions

The RERTR-7A breach occurred at very high burnup near the end of the planned irradiation test immediately after being exposed to the rapid thermal transient that accompanies an unplanned reactor scram. It is likely that the cladding of several mini-plates was stressed at this time due to the swelling that has been observed in some of the experimental fuel meat compositions. When coupled with the large stresses induced by the thermal transient it is believed that a cladding rupture occurred, exposing the fuel meat to primary coolant. Compositional analysis of the primary coolant, stack gas composition analysis, and soak testing proved to be useful tools in the diagnosis of the breach. Additional detailed analysis of the mini-plate behavior in the breached condition will be documented separately during PIE of the failed capsule and its contents.

3. RERTR-8 Irradiation Test

The RERTR-8 experiment will build on the experience gained and lessons learned from the previous seven RERTR mini-plate irradiation campaigns. This experiment will be used to further examine and understand ways to control detrimental fuel/matrix interactions, evaluate fundamental irradiation behavior of various fuel compositions, and to explore advanced fabrication techniques. The results will be used to support the selection of fuel compositions promising enough to carry into full-size plate irradiations. This experiment also marks a transition from feasibility tests to more focused tests that are intended to start generating the data required for the eventual qualification documentation that will be supplied regulators.

The development of dispersion and monolithic fuel types will continue to be carried out in parallel. The particular performance challenges associated with each are somewhat reflected in the goals/objectives described below for each aspect of the RERTR-8 experiment. It is important that the experiment be designed to allow direct comparison of various parameters that will lead to meaningful quantitative and qualitative understanding of the phenomena being tested. This requirement will be reflected in both the composition and configuration of the experiment.

3.1 Summary of Experiment Objectives

The experiment objectives are summarized below. A more detailed justification is given for each fuel type in the following sections.

- Continue development of advanced fuel technologies for high power reactors (i.e. HIFR, FRM-2, etc.). Initial efforts will be focused on the demonstration of fuel with burnable poisons.
- Evaluate the performance of fuel meats based on a magnesium matrix.
- Demonstrate fabrication of monolithic fuel plates using HIP.
- Evaluate monolithic plate swelling as a function of Mo content in the fuel alloy (e.g. compare U-8Mo, U-10Mo, and U-12Mo).
  Extend experience with ternary dispersion fuel alloys by irradiating Zr and Ti bearing plates to higher burnup than RERTR-7B.

3.2 Dispersion Fuels

U-Mo based dispersion fuels have been plagued by excessive swelling (in some cases breakaway swelling) that is driven by the formation of unstable $(U,Mo)Al_x$ phases during irradiation. Two fundamental approaches to limiting this behavior were proposed and explored in the RERTR-7 series of experiments. The addition of silicon to the matrix and the addition of zirconium or titanium to the fuel

phase were expected to limit the formation of higher aluminides (x=7), which are assumed to be the source of instability during irradiation. Several matrix compositions were explored in the RERTR-6 and -7A experiments including Al-0.2 Si, Al-2.0 Si, Al-6061, and Al-4043. The RERTR-6 experiment subjected the plates to moderate powers (surface heat flux ~140-175 W/cm^2), high temperature (centerline temperature at BOL ~116-180ºC), and were irradiated to moderate burnup (~50% LEU). The RERTR-7A experiment subjected the plates to high power (surface heat flux ~215-325 W/cm^2), high temperature (centerline temperature at BOL ~120-165ºC), and high burnup (~60-90% LEU equivalent). Preliminary PIE data from the RERTR-6 and –7 experiments indicates that higher Si content in the matrix reduces net plate swelling and fuel/matrix interaction thickness. The use of ternary fuel alloys was also proposed to perform the same function. Small additions of zirconium (2%) and titanium (1%) were incorporated into the fuel alloy of plates tested in the RERTR-7B experiment where they were subjected to high power (surface heat flux ~190-235 W/cm^2), high temperature (centerline temperature ~110-125ºC) and moderate burnup (25-30% LEU equivalent). PIE is being performed on these plates along with the RERTR-7A experiments. More recent analytical studies have suggested that higher ternary content will be required to yield the desired affect.

The impact of adding zirconium or titanium to the fuel alloy on the interaction layer behavior during irradiation will also be examined in the RERTR-8 experiment. The U-7Mo-1Ti and U-7Mo-2Zr fuel alloy was evaluated to moderate burnup in the RERTR-7B experiment and will be carried to higher burnup (~70% LEU equivalent) in the RERTR-8 experiment. A high silicon matrix material (Al-4043) will be used in both plates.

A performance of a U-7Mo fuel alloy dispersed in a magnesium matrix will also be evaluated. Although early tests of this composition were performed on 'nano-plates' during the RERTR-3 experiment, the RERTR-8 plate will be first at the mini-plate scale. As a precautionary measure, the plate will be located in the D-capsule by itself and will be removed after one irradiation cycle (~30% LEU equivalent burnup).

U_3Si_2 based dispersions will be included in the experiment to act as control plates.

3.3 Monolithic Fuels

Irradiation performance data for monolithic fuels, although limited, has been promising. Monolithic fuels eliminate the entire matrix component and minimize the fuel alloy/aluminum interfacial area and temperature. It is also significant that the monolithic fuel form may be the only path to converting many of the high power reactors currently targeted (including HIFR, FRM-2, and ATR) by the GTRI. These reactors will require a complex fuel with tailored fuel grading and the incorporation of burnable poisons. Fabrication poses a significant challenge for the basic monolithic fuel form and, consequently, several techniques are currently being pursued including friction stir welding (FSW), transient liquid phase bonding (TLPB), and hot isostatic pressing (HIP). Both FSW and TLPB have been used to successfully fabricate plates used in the RERTR-6 and -7A experiments. Preliminary study was performed on monolithic fuel plates in the RERTR-4, -6, and -7A experiments where U-7Mo, U-10Mo, and U-12Mo based fuels have been tested. U-7Mo and U-10Mo fuels were irradiated to moderate burnup (~45%) at high temperature (~125-205ºC) and moderate power (surface heat flux ~165-225 W/cm^2) during the RERTR-6 experiment. U-10Mo and U-12Mo fuels were irradiated to high burnup (~50-83%) at high temperature (centerline temperature ~100-146ºC) and power (surface heat flux ~165-300 W/cm^2) in the RERTR-7A experiment. PIE of the RERTR-6 experiment indicated that plate swelling increased as the molybdenum content in the fuel alloy dropped.

The RERTR-8 experiment will evaluate the relative swelling of plates as a function of molybdenum content in the fuel alloy by directly comparing U-7Mo, U-8Mo, U-10Mo, and U-12Mo based plates. The experiment will also explore the feasibility of advanced fabrication techniques and processes. The HIP process was successfully used to fabricate plates with molybdenum content of at least 10wt%, while FSW was used for lower alloys to limit fuel/clad interaction during fabrication. The irradiation performance of U-10Mo monolithic plates fabricated by both techniques will be evaluated as well. A plate was also fabrication with a layer of borated aluminum attached to the fuel foil to demonstrate the incorporation of burnable poison into monolithic fuels.

3.4 Experiment Configuration

The standard RERTR mini-plate hardware for ATR Large B-Position irradiations will be used for this experiment. The irradiation basket will be unorificed to maximize coolant flow. To limit the risk of a cladding breach similar to that seen in the RERTR-7A experiment, peak burnup will be limited to ~75% LEU equivalent. This can be accomplished without any experiment modifications or capsule shuffling by using the West Large B-Position (B-12) of the ATR for at least one irradiation cycle. Comparison of RERTR-7A (B-11) and -7B (B-12) burnup in cycle 136B shows that the rate of depletion in B-12 is roughly 2/3 that of B-11. Peak burnup after one cycle in B-11 and one cycle in B-12 (~100 EFPDs total) should be on the order of 75% LEU equivalent (when using 58% enriched uranium).

The experiment was inserted into the ATR on October 13, 2006 for cycle 138A. The experiment matrix is shown in Table 9. The peak beginning of life thermal conditions for the experiment are shown in Table 10. To provide low burnup performance data on the magnesium matrix fuels, capsule D will be removed from the RERTR-8 experiment and replaced by a dummy capsule after one cycle. The capsule will be stored in the ATR canal during the second cycle and will be shipped with the rest of the experiment. The experiment will be completed in February 2007 and PIE should be initiated in late April.

RERTR-8 Experiment Matrix				
Capsule	**Column 1**	**Column 2**	**Column 3**	**Column 4**
A-Top	A1 U_3Si_2 Al U0R60	A2 U-10Mo FSW 0.01Ó fál LIF200	A3 U-7Mo-1Ti Al-4043 D3R040	A4 U-7Mo-2Zr Al-4043 F3R030
A-Bottom	A5	A6	A7	A8
B-Top	B1	B2	B3	B4
B-Bottom	B5 U-12Mo HIP 0.01Ó fál/BorAl H1P02B	B6	B7	B8
C-Top	C1 U-10Mo HIP 0.01Ó fál L1P020	C2 U-8Mo FSW 0.01Ó fál J1F020	C3 U-10Mo FSW 0.01Ó fál LIF190	C4 U-12Mo HIP 0.01Ó fál H1P010
C-Bottom	C5 U-7Mo-1Ti Al-4043 D3R030	C6 U_3Si_2 Al U0R040	C7 U-7Mo Al-4043 R3R060	C8 U-7Mo-2Zr Al-4043 F3R040
D-Top	D1	D2 U-7Mo Mg Matrix R9R010	D3	D4
D-Bottom	D5	D6	D7	D8

Table 9. RERTR-8 experiment matrix.

Fuel Plate	Fuel Type	Fuel Form	Heat Flux (W/cm2)	Fuel Plate Power (W)	Coolant Temp (°C)	Plate Surf. Temp (°C)	Clad Surf. Temp (°C)	Fuel-Clad Inter Temp (°C)	Fuel Cent Temp (°C)
A-1	U3Si2	disp	162	5860	53	76	80	84	101
A-2	U-10Mo	foil	130	4684	53	72	75	79	86
A-3	U-7Mo-1Ti	disp	144	5187	53	74	77	80	96
A-4	U-7Mo-2Zr	disp	152	5495	53	75	78	82	98
A-5	blank	-n/a-	0	0	55	55	55	55	55
A-6	blank	-n/a-	0	0	55	55	55	55	55
A-7	blank	-n/a-	0	0	55	55	55	55	55
A-8	blank	-n/a-	0	0	55	55	55	55	55
B-1	blank	-n/a-	0	0	55	55	55	55	55
B-2	blank	-n/a-	0	0	55	55	55	55	55
B-3	blank	-n/a-	0	0	55	55	55	55	55
B-4	blank	-n/a-	0	0	55	55	55	55	55
B-5	U-12Mo w/ BorAl	foil	307	11090	57	101	107	118	134
B-6	blank	-n/a-	0	0	57	57	57	57	57
B-7	blank	-n/a-	0	0	57	57	57	57	57
B-8	blank	-n/a-	0	0	57	57	57	57	57
C-1	U-10Mo	foil	244	8812	59	94	100	109	121
C-2	U-8Mo	foil	233	8416	59	93	98	106	118
C-3	U-10Mo	foil	216	7783	59	90	95	103	114
C-4	U-12Mo	foil	242	8736	59	94	99	108	120
C-5	U-7Mo-1Ti	disp	243	8767	63	98	103	109	135
C-6	U3Si2	disp	241	8699	63	98	103	109	134
C-7	U-7Mo	disp	230	8303	63	96	101	107	131
C-8	U-7Mo-2Zr	disp	245	8828	63	98	104	110	135
D-1	blank	-n/a-	0	0	66	66	66	66	66
D-2	U-7Mo	disp	299	10795	66	109	115	123	154
D-3	blank	-n/a-	0	0	66	66	66	66	66
D-4	blank	-n/a-	0	0	66	66	66	66	66
D-5	blank	-n/a-	0	0	67	67	67	67	67
D-6	blank	-n/a-	0	0	67	67	67	67	67
D-7	blank	-n/a-	0	0	67	67	67	67	67
D-8	blank	-n/a-	0	0	67	67	67	67	67

Table 10. RERTR-8 beginning of life, nominal thermal conditions.

4. Full-Size Plate (AFIP-1) Irradiation Test

The next phase in the fuel qualification plan is to extend testing of promising mini-plate fuel compositions to plates of near prototypic dimensions (i.e. “full-size” plates). This series of tests, dubbed the AFIP (**A**TR **F**ull-size plate **I**n center flux trap **P**osition) experiments, will require an irradiation position much larger than the Large-B positions used for mini-plate testing. Conceptual design of irradiation test hardware for the ATR Center Flux Trap (CFT) (see Figure 14) is nearly complete and irradiation is scheduled to begin in March 2006.

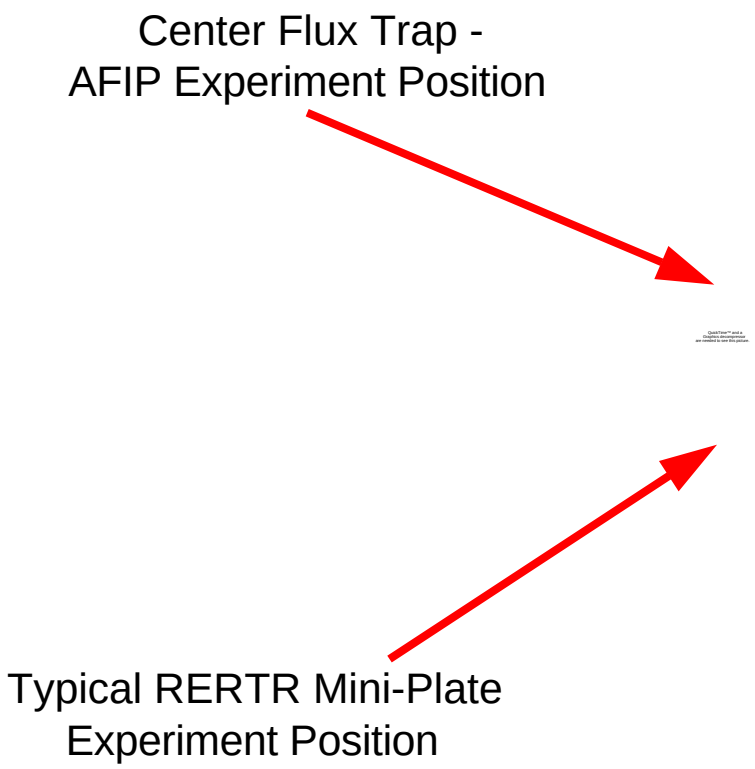

Figure 14. AFIP and mini-plate experiment positions in the ATR.

The experiment will accommodate four plates roughly 24’ x 3” x 0.050”. Two dispersion and two monolithic plates will be irradiated in the experiment. Extension of the dispersion fuel plates from the mini-plate to full-size scale is not expected pose significant irradiation performance issues (although fabrication may), monolithic fuels however are much less mature and issues associated with scale may be more important. As a result, the dispersion plates will be operated at higher power (~310 W/cm^2 peak surface heat flux) than the monolithic (~260 W/cm^2 peak surface heat flux). This will be accomplished by loading the dispersion fuel plates with 25% enriched uranium and the monolithic fuel plates with 20% enriched uranium. The experiment will be subjected to two irradiation cycles in the ATR and should reach peak burnups of near 70% LEU equivalent. Profilometry and ultrasonic scans will be preformed on each plate to evaluate swelling and the fuel/clad interface before and after each cycle.

The AFIP plates are held in aluminum frames that will provide rigidity during examination and reduce the risk of damage during handling. The AFIP plate frame will be comprised of two 0.25-inch square 6061-T6 aluminum flats (referred to as “rails”) that have slots cut in one side, along their entire 48.75-inch length. The plate frame houses two AFIP fuel plates stacked vertically and are bound by 0.050-inch thick 6061-T6 aluminum sheet segments, used for plate frame handling and structural frame support. The fuel plates and aluminum sheet segments are placed between the two slotted rails and welded into place, leaving two 0.5-inch thermal expansion gaps between fuel plate top and bottom edges and aluminum sheet segments. Mating edges of the two fuel plates are welded to side rails at mid-

length, thus allowing for unrestrained thermal expansion of fuel plates within rail slots. Figure 15 shows a conceptual design representation of the AFIP plate frame assembly.

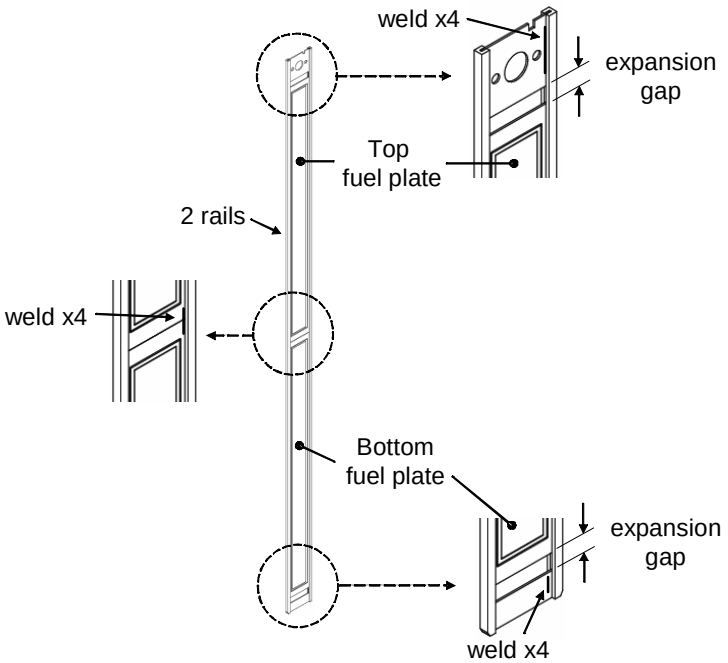

Figure 15. AFIP test plate schematic.

The AFIP plates and their frames will be inserted into the AFIP plate holder, which will be comprised of a 3.125-inch diameter 6061-T6 aluminum cylinder that is 60.33-inches in length. The plate holder has a rectangular hole that extends through most of its annulus that serves as a cavity for two plate frame assemblies and other support components. Four additional holes (or slots) have been cut along the holder's perimeter length allowing for placement of four flux wire monitors that will be used to evaluate the neutronic conditions of the experiment. The top of the plate holder has a 0.125-inch thick lip that extends 4-inches tangent to the cylinder's side and has features for lifting and handling the plate holder. The bottom of the plate holder has features that interface to existing center flux trap equipment, which is used to align and orient the plate holder (and its contents) within the ATR reactor center position. When fully-loaded, the plate holder contains two plate frame assemblies, ram, ram-rod, and four flux wire monitors. The ram and ram-rod components are use to provide dimensional spacing and structural support to the two plate frame assemblies within the holder. A flow orifice will be attached to the holder exit to control hydraulic conditions in the assembly. Figure 16 shows a conceptual design representation of the AFIP plate holder and its contents.

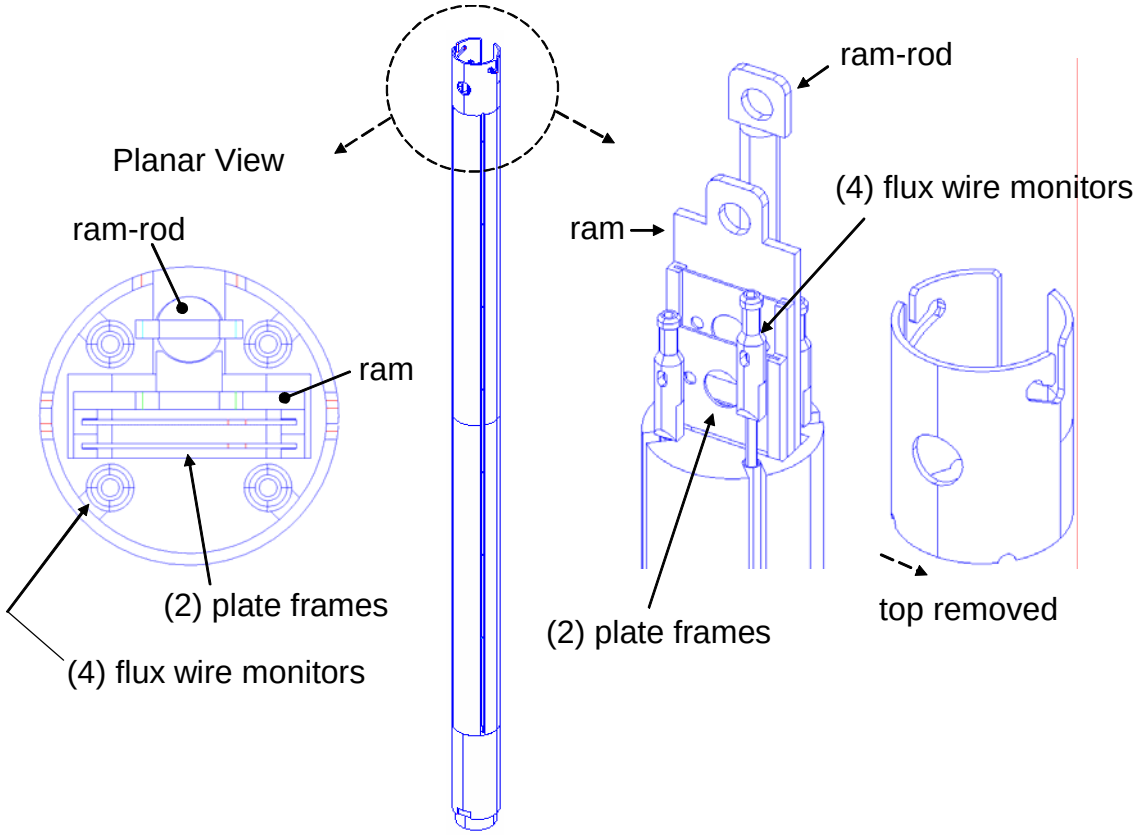

Figure 16 – Conceptual design representation of the AFIP plate holder assembly, when loaded.

Future full-size plate tests are also planned. The AFIP-2 experiment is planned to include both monolithic and dispersion fuel plates. The monolithic fuel plates will be combination of higher power fabricated by friction stir welding (FSW) and/or hot isostatic pressing (HIP). The HIP plates will be fabricated at BWXT using foils fabricated at Y-12. The FSW plates will be fabricated at Idaho National Laboratory. The dispersion plates will be fabricated with higher fuel loadings (~8 g-U/cc) or slight variations in matrix composition from the AFIP-1 test. These plates will be fabricated at Argonne National Laboratory. Follow on tests will be designed to evaluate advanced fuel concepts (i.e. graded fuel) for special purpose reactors like HFIR.

5. Conclusions

Irradiation testing is being conducted as a central component of fuel development for the RERTR program. Tests continue to be carried out at the mini-plate scale in order to develop a comprehensive understanding of the fuel's thermo-chemical behavior. The RERTR-7A and RERTR-7B experiments were recently completed and are being examined. These tests are expected to complete the feasibility stage of the fuel development (assuming continued positive results from PIE). Two plates in the RERTR-7A experiment experienced a cladding breach. The cause of the breach is still being evaluated. The RERTR-8 experiment was recently inserted into the ATR and marks a transition from a feasibility stage to the initial stages of fuel qualification. Effects of scale-up will be evaluated in full-size plate test. It is expected that the thermo-mechanical behavior at full-scale may be different than at the mini-plate scale, especially for the monolithic fuel. A more aggressive path to qualification is possible for dispersion fuels since issues of scale are reasonably well defined. Monolithic fuel will require a more deliberate approach that gradually exposes the fuel to more aggressive conditions to identify and evaluate potential failure modes.

6. References

1. Failed Fuel Action Plan Guidelines, Palo Alto, CA: Electric Power Research Institute, November 1987, EPRI NP-5521-SR.
2. Lin, C. C., Radiochemistry in Nuclear Power Reactors, National Academies Press, 1996